



## **Intelligent switching between different noise propagation algorithms: analysis and sensitivity**

Eric Boeker<sup>a)</sup>

Environmental Measurement and Modeling Division

United States Department of Transportation, John A. Volpe National Transportation Systems Center  
Cambridge, MA 02142

Joyce Rosenbaum<sup>b)</sup>

Computer Sciences Corporation

Cambridge, MA 02142

**When modeling aircraft noise on a large scale (such as an analysis of annual aircraft operations at an airport), it is important that the noise propagation model used for the analysis be both efficient and accurate. In this analysis, three different propagation methods are compared over a range of different environmental conditions (uneven terrain, terrain blockage, refractive atmosphere, and ground type transitions) and geometric orientations. These results are then used to inform a scheme of “intelligent switching” between different noise propagation methods as an approach to address the long computational runtimes without sacrificing accuracy in a noise model. The feasibility of this strategy is discussed and potential implementation hurdles are identified.**

### **1 INTRODUCTION**

The Volpe National Transportation Systems Center and the Federal Aviation Administration (FAA) are in the process of investigating enhancements to the modeling capabilities of the FAA’s Aviation Environmental Design Tool (AEDT) and Integrated Noise Model (INM) in complex environments, such as National Parks. This research has led to the development of the hybrid propagation model (HPM), a numerical model designed to predict aviation noise levels under complicated propagation conditions. HPM was originally developed through a cooperative research effort with the Pennsylvania State University<sup>1,2</sup>. HPM is a composite of three propagation methods: a parabolic equation (PE) model; a fast field program (FFP); and a straight ray-trace model.

The three component models of the HPM were chosen for their complementary strengths. The PE allows the HPM to incorporate range-dependent effects at small elevation angles from

---

<sup>a)</sup> email: Eric.Boeker@dot.gov

<sup>b)</sup> email: Joyce.Rosenbaum.CTR@dot.gov

the source, such as terrain features, transitions between different types of ground, and changing meteorology. The FFP ensures that the model is accurate at low frequencies to moderate elevation angles, for cases without extreme range-dependent changes near the source. The straight-ray model fills in levels at the higher elevation angles, where the accuracy of the other two models is degraded. The resulting HPM can return noise levels at all points in the vertical, line-of-sight slice between the source and a distant receiver. The full HPM has the longest runtime, followed closely by the FFP, while the ray model is by far the fastest. This paper presents a study of various propagation conditions run by HPM and its component models. Comparisons are made between the full HPM, a pure FFP, and a pure ray model. Analyses of the more complicated propagation conditions provide a foundation upon which to develop potential criteria for reducing computation time of noise level predictions by identifying conditions that do not demand the advanced capabilities of the full HPM, but rather can afford to be run by a simpler, faster method. A detailed comparison of these cases reveals how the HPM and its component models could be utilized most efficiently. Once further refined, optimized and validated, the HPM could be integrated into AEDT, to handle modeling more complex noise propagation conditions.

## 2 OVERVIEW OF THE NOISE MODELS

The PE model used in the HPM is a two-dimensional generalized terrain, finite difference formulation<sup>3,4,5</sup>. It is derived from the one-way Helmholtz equation<sup>5</sup> with use of an assumption that limits the validity of the model to elevation angles up to approximately  $\pm 35$  degrees from the horizontal of the source. The PE propagates sound in the two-dimensional vertical plane by extrapolating results at one range step from results at previous range steps, and it incorporates range-dependent effects at small elevation angles from the source, such as terrain features, transitions between different types of ground, and changing meteorology. However, because it is derived from the one-way Helmholtz equation, it can only account for sound moving in the forward direction from the source to the receiver and does not include backscatter.

Because of the elevation angle limitation of the PE, the HPM utilizes the FFP in conjunction with the PE. The FFP<sup>5,6,7</sup> is derived from the Helmholtz equation by applying a transformation from the horizontal spatial domain into the horizontal wave number domain. It propagates sound in the two-dimensional vertical plane between stratified layers of the atmosphere. The FFP, accurate both at low frequencies and at moderate elevation angles, supplements the PE. However, it is limited to inclusion of non-range-dependent propagation effects, and errors are introduced at higher elevation angles from the effects of a window applied in the horizontal wave number domain. The valid angle range depends on the steepness of the window roll-off. The window used in the calculations of this report introduces inaccuracies at angles above 72 degrees. However, to be conservative, a smaller angle range below 48 degrees was used.

Finally, a straight-ray model is used to fill in the regions of the steepest emission angles from the source. This model is a superposition of the direct and reflected sound at the receiver point, assuming the sound follows a straight path. While it can include the effects of a uniform, finite-impedance ground, it incorporates neither range-dependent effects, nor refractive atmospheres. More advanced ray models, however, are able to incorporate these propagation effects. The straight-ray model was used in this research for the smallest ranges, where range-dependent effects will have a minimal effect.

The construction of the hybrid model is achieved by joining the ray, FFP, and PE components in the appropriate regions in the two-dimensional vertical plane, as shown in Figure 1. PE results are used in elevation angles of 35 degrees and below, FFP results are used between

35 and 48 degrees, and ray results are used above 48 degrees. The performance of both individual PE and FFP models was verified against both analytical solutions and published results<sup>5,8</sup>. The ray model was verified against the PE and FFP models. Merging them into a hybrid model is validated in this report through running test cases that explore results of different source heights and frequencies, as well as propagation conditions.

### **3 MODEL COMPARISON**

Ten different test cases are considered in this analysis. A base case is presented first (Case 1) as a control condition for the remaining cases. The base case includes a flat, soft ground and a homogeneous atmosphere. The next 9 cases each isolate a single propagation mechanism and consider its effect on the base case results. Case 2 uses a hard, flat ground and a homogeneous atmosphere; Cases 3 and 4 use a soft, flat ground with an upward and downward refracting atmosphere, respectively; Cases 5, 6, and 7 use a soft ground with a hill, upward sloping, or downward sloping ground, respectively, and a homogeneous atmosphere; Cases 8 and 9 use transitions from hard to soft ground, or soft to hard ground, respectively, with flat terrain and a homogeneous atmosphere; Case 10 uses two ground-type transitions, first from hard to soft ground and then back to hard ground, with flat terrain and a homogeneous atmosphere. The mechanisms can be broken into three categories of effects: ground type, terrain, and meteorology.

Diagrams of the geometries of each case are shown in Figure 2. Green lines indicate soft ground and brown lines indicate hard ground. Each condition consists of a point source at a given altitude. Sound speed profiles for each case are also shown in Figure 2. Results are presented as a function of horizontal range from the source for a receiver at a given height above the ground. Four source heights are considered for each case. The common parameters are presented in Table 1.

#### **2.1 Base Case: Soft, Flat Ground, Homogeneous Atmosphere**

Case 1 uses the simplest set of propagation conditions: a soft, flat ground with a homogeneous atmosphere. It serves both as a starting point of comparison between the component models, and between the four different source height conditions, and also as the baseline for evaluating the added effects of more complicated mechanisms in propagation.

Figure 3 shows results for Base Case 1, separately, for the 4 different source heights. Each subfigure plots HPM, FFP, and ray model results. HPM results are composed of ray results at the smallest ranges, then FFP results for the moderately small ranges, and PE results for the remainder of the range. The FFP and ray results are calculated exclusively with the FFP and ray models, respectively. The results presented are A-weighted maximum sound levels, and the combination of the twenty-four one-third octave band results smoothes the severe interference pattern peaks and dips of the individual frequency bands.

Aside from results at the smallest ranges, where the FFP accuracy is degraded, the results of the three models agree well and the plotted HPM, FFP, and RAY result lines are nearly indistinguishable. For this simple set of propagation conditions—soft, flat ground and a homogeneous atmosphere—the agreement between the three models indicates that, so long as the model is considered to be accurate in the propagation region of interest, the choice of model is insignificant.

#### **2.2 Effect of Ground Type**

Case 2 is similar to Case 1, but uses hard ground in place of soft. Again, results of the three models (HPM, FFP, and ray) agree well in the region where all models are valid, indicating that the choice of model is unimportant, as long as the model is considered to be accurate in the propagation region of interest. Consequently, agreement between the HPM, FFP, and ray models under purely soft or hard ground conditions allows the HPM curve to be used as a surrogate for any of the three models in comparisons with these cases. Therefore, Figure 4 presents a comparison of HPM results for soft ground, hard ground, and a hard to soft ground transition, Cases 1, 2, and 8, respectively, for each source height. Because neither the FFP or ray model takes into account range-dependent effects, only the HPM results are used to analyze the propagation effect of the ground type transition.

Relative agreement of the three curves shows ground type to have a fairly minimal effect at small ranges (less than approximately 400 m for the geometries explored in this paper). In addition, Case 8 hard to soft ground transition results are equal to Case 2 at the smaller ranges where propagation is over hard ground. At the transition to soft ground, results diverge from the Case 2, hard ground results, and approach Case 1, soft ground, results.

Similar results were observed for Case 9, where the ground type transitioned from soft to hard ground, and for Case 10, where the ground type transitioned from hard to soft ground at 600 m and then back to hard ground at 1800 m.

### 2.3 Effect of Refractive Atmosphere

Case 3 differs from Case 1 in its applied atmospheric conditions. An upward refracting atmosphere, used in Case 3, can result either from wind (in upwind conditions) or from a negative thermal gradient (in daytime conditions when air temperature decreases with height). Equation (1) defines the logarithmic refracting atmosphere used in this analysis

$$c(z) = c_0 + b \ln\left(\frac{z}{z_0} + 1\right), \quad (1)$$

where  $c_0$  is the sound speed at the ground equal to 340.2 m/s,  $b$  is the logarithmic sound speed profile parameter equal to -1 m/s,  $z_0$  is the aerodynamic roughness length of the ground surface equal to 0.1 m, and  $z$  is the height above the ground.

Figure 5 shows the comparison between HPM and FFP results for each source height. The ray model is not included because it was not developed to incorporate a refractive atmosphere. However, the HPM Case 1 results, which are similar to the ray model results for baseline conditions and are the closest conditions to Case 3 achievable by the ray model, are included for comparison.

While levels are similar between Cases 1 and 3 at the smaller ranges, severe drops in level are observed in Case 3 for the lowest three sources. This drop occurs when the receiver enters the shadow zone, regions into which rays cannot reach. For all sources, there is a slight increase in level just before the shadow zone, caused by the slight focusing of the remaining sound being directed upward.

The HPM and FFP results agree well after the smallest ranges and before the shadow zone has formed. Once levels drop below approximately 50 dB, the HPM and FFP results deviate slightly, with larger levels predicted by the HPM.

Case 4 uses a downward refracting atmosphere with a logarithmic sound speed profile parameter of  $b$  equal to 1 m/s. A downward refracting atmosphere occurs in downwind conditions and during nighttime hours when the ground cools faster than the atmosphere and the temperature of the air increases with height above ground. Figure 6 shows the comparison between HPM and FFP results for each source height. HPM and FFP agree well beyond the smallest range values. The downward refracting atmosphere results show lower levels than Case 1 at small ranges and higher levels than Case 1 at the longer ranges, for the lowest two source altitudes. Levels increase at larger ranges, where the sound has bent back toward the ground contributing to multiple ray arrivals. The effect of additional arrivals is seen in the jaggedness of results for the lowest altitude source.

## 2.4 Effect of Terrain Blockage

Case 5 introduces the effects of a terrain feature on propagation. Figure 7 shows the HPM results for propagation over a hill for each source height. The FFP and ray models are not included because neither incorporates range-dependent effects. However, Case 1 results are shown for comparison.

Because the model does not account for backscattering off obstacles, Case 5 results agree exactly with Case 1 until the horizontal range of 800 m, where the hill begins. For the three lowest sources, the level increases over the incline portion of the hill, as the sound interacts with the upslope. Beyond the crest of the hill, where the line of sight between source and receiver is obstructed, there is a large drop in level. However, the level increases again over the end of the hill, and continues to increase into the second flat ground region, due to diffraction.

Results for the highest altitude source (400 m) agree well with Case 1, except over the downslope of the hill. Here, even though the line of sight between source and receiver is never fully broken, the direct ray passes very close to the ground. The reflected ray, therefore, meets the ground at a shallow angle, which can introduce a more significant ground effect than in the flat ground in Case 1. This effect could explain the small dip in Case 5 results for the 400 m source height over the downslope of the hill.

Case 6 represents an upward sloping terrain feature. Figure 8 shows the HPM results for each source height. Because the propagation conditions of Case 6 are identical to those of Case 5 until the top of the upward slope at 1200 m range, the results of the two cases are equal to this point. Beyond the crest of the sloped ground, a shadow zone formed by obstruction of the line of sight by the terrain feature only exists for the lower two source altitudes, and these shadow zones are less severe, reflected in the milder level decrease in noise levels.

Despite the absence of a line of sight blockage for the 100 m source, the upward sloping terrain does have an effect on results at larger ranges of propagation. An increase in ground effect is caused by the shallower angle of reflection of the ray off the ground, due to the raised terrain. The results of the 400 m source height, for which there is no line of sight blockage, and for which the angle of reflection of sound with the ground is still fairly steep, agree well with Base Case 1 over the full range.

Case 7, not shown, representing a downward sloping terrain feature, also experiences dips in level caused by a line of sight blockage. The shapes of the dips resemble results for Case 5 beyond the peak of the hill, but are not as extreme. In this case, the vertical height difference between the sources and receivers is larger because the sources were placed with respect to the raised terrain. The steeper elevation angles between sources and receivers cause a milder obstruction by the terrain feature. Again, an increase in level caused by diffraction is observed over the end of the downslope, continuing over the flat ground.

### 3 ANALYSIS FOR INTELLIGENT SWITCHING

The comparisons between the results of the ten different cases discussed in this report help determine the appropriateness of “intelligent switching” for aircraft noise modeling. The idea of a hybrid model utilizing alternative noise propagation methodologies to fill in regions where the PE model was not valid, and ensure full coverage for an aircraft noise model, was central to the development of the HPM. The goal of this analysis is to make further use of the propagation models available by design within the HPM to refine intelligent switching criteria that identify instances where a detailed propagation model is necessary to capture all significant effects, and other instances where a simpler (and faster) model may be sufficient.

All three models (HPM, FFP, and ray) were found to return nearly equivalent results for the simplest propagation conditions in Cases 1 (baseline, soft ground) and 2 (hard ground). The agreement of the three HPM component models under these conditions not only provide further confirmation of the correctness of the model implementations, as checks against each other, but also justifies utilization of the intelligent switching concept, by which component models may be chosen as surrogates for the full HPM in order to reduce runtimes. As an example, Case 1 took over two days to run with the HPM and slightly under two days to run with just the FFP. In contrast, the ray model ran Case 1 in less than a minute. Such a large decrease in runtime is extremely valuable. Still, the ray model is slower than the INM, which takes only seconds to run. Cases 1 and 2 provide proof of concept that at least two sets of propagation conditions are ideal candidates for a “switch” to use of the ray model in place of the full HPM.

Case 3 (upward refracting atmosphere) showcased scale of effects certain propagation mechanisms can have on overall reported levels; from large drops in level observed inside shadow zone regions, to small increases in level before the start of the shadow zone. In Case 4 (downward refracting atmosphere), multiple arrivals from sound reflected off the ground more than once cause increased levels at larger horizontal propagation ranges. However, while inaccurate results would be returned by a model incapable of including atmospheric effects, such as our straight-ray model, the FFP shows fairly good agreement with the full HPM results, especially in the beginning portion of the shadow zone, where levels are decreased, but still likely audible. Thus, Cases 3 and 4 suggests that, for refracting atmospheric conditions, care must be taken inside a shadow zone and at ranges that support more than two (direct and single reflection) paths from source to receiver. The FFP can be used in place of the full HPM to save a small amount of runtime.

Case 5 (hill), Case 6 (upward sloping terrain) and Case 7 (downward sloping terrain) clearly demonstrate the effect of a line of sight blockage between a source and receiver. A large drop in level is observed following the initial obstruction of the direct path, while diffraction increases the attenuated levels both over the end of the terrain feature and into the flat region beyond. In addition, there is an increase in level over the inclined portion of terrain for the lower altitude sources. While the absence of line of sight blockage for the highest altitude source does cause levels to show little effect of the terrain feature for the majority of the propagation range, an effect of shallow angle of reflection off the ground causes a small dip in level over the back of the terrain feature. Thus, Cases 5 to 7 suggest that, when the dimension of the terrain feature are small compared to the source altitude, and the line of sight between source and receiver is not broken, the effect of a terrain feature is greatly diminished. Because the ray model, FFP, and HPM results all agree for simple propagation conditions like Case 1, and because the terrain cases results for the high altitude source agree well with Case 1 results, a switch from the full HPM to one of the simpler models could be employed. However, if a simpler propagation method, such as the straight-ray model, is to be substituted for the full HPM, care must also be

taken to ensure a minimum steepness of the sound reflected off the ground at all points in range. If differences between the full HPM and the simple ray model do exist, they would be seen near the terrain feature.

Case 8 (hard to soft ground transition), Case 9 (soft to hard ground transition), and Case 10 (hard to soft and soft to hard ground transitions) reveal a few points of caution and also a few instances of support for intelligent switching. In these cases, it was found that the effect of a transition of ground type can be significant for a low altitude source out to long ranges. However, for fairly high altitude sources, the effect of the previous ground type on the results at a receiver placed after the transition does not last long. This suggests that, if the receiver is far enough from the transition point, a single ground impedance input reflecting the type of ground directly beneath the receiver is sufficient. Thus, for high altitude sources for which angles of ground reflections are steep enough, the straight-ray model can be substituted for the full HPM at most points in range.

## **4 CONCLUSIONS**

Ten different sets of propagation conditions were run with the HPM and its component FFP and ray trace models for four different source heights, using an aircraft spectrum. The results of the cases were analyzed and compared to provide insight into the effects of the different propagation mechanisms on noise level predictions. In order to advance the concept of “intelligent switching” between the component models and full version of the HPM, focus was placed on identifying conditions that did not require use of the full HPM and potentially reduced computational time.

It was found that there are potential opportunities for the use of a single, faster component model, in place of the full HPM. The straight-ray model could be used under simple propagation conditions with a homogeneous atmosphere and finite impedance ground, without range-dependent effects. The FFP model could be used under refractive atmosphere conditions without range-dependent effects. Even further, for higher altitude sources, the impact of range-dependence effects often becomes negligible, and the ray model or FFP could be substituted, despite their failure to include range-dependent effects. However, certain points of caution are offered to avoid applying a simpler model where the full model is needed. The major categories for which care should be taken before applying a simpler model include line of sight obstructions between source and receiver, shallow angles of reflection off the ground, and close proximity to ground impedance transitions.

Overall, this analysis provides a foundation upon which to develop potential criteria for reducing computation time of noise level predictions by identifying conditions that do not demand the advanced capabilities of the full HPM, but rather can afford to be run by a simpler, faster method. With further analysis and validation, the HPM could be refined and optimized to best use “intelligent switching” methods and eventually integrated into AEDT, to handle modeling more complex noise propagation conditions.

## **5 ACKNOWLEDGEMENTS**

We gratefully acknowledge the support of the FAA Office of Environment and Energy, FAA Western-Pacific Region, and the National Park Service (NPS) Natural Sounds and Night Skies Division.

## 6 REFERENCES

1. Rosenbaum, J. E., A. A. Atchley, and V. W. Sparrow, “Enhanced sound propagation modeling of aviation noise using a hybrid Parabolic Equation-Fast Field Program method,” Inter-Noise conference proceedings, Ottawa, ON (2009).
2. Rosenbaum, J. E., “Enhanced propagation modeling of directional aviation noise: A hybrid parabolic equation-fast field program method,” Ph.D. dissertation, The Pennsylvania State University (2011).
3. West, M., K. Gilbert, and R. A. Sack, “A tutorial on the parabolic equation (PE) model used for long range sound propagation in the atmosphere,” *Applied Acoustics*, 37(1), 31-49.
4. Sack, R. A., and M. West, “A parabolic equation for sound propagation in two dimensions over any smooth terrain profile: the generalized terrain parabolic equation (GT-PE),” *Applied Acoustics*, 45(2), 113-129 (1995).
5. Salomons, E. M., *Computational Atmospheric Acoustics*, Kluwer Academic Publishers (2001).
6. Franke, S. J. and G. W. Swenson, Jr., “Brief tutorial on the Fast Field Program (FFP) as applied to sound propagation in the air,” *Applied Acoustics*, 27(3), 203-215 (1989).
7. West, M., R. A. Sack, and F. Walkden, “The Fast Field Program (FFP). A second tutorial: Application to long range sound propagation in the atmosphere,” *Applied Acoustics*, 33(3), 199-228 (1991).
8. Attenborough, K., S. Taherzadeh, H. E. Bass, X. Di, R. Raspet, G. R. Becker, A. Güdesen, A. Chrestman, G. A. Daigle, A. L’Espérance, et al., “Benchmark cases for outdoor sound propagation models,” *J. Acoust. Soc. Am.*, 97(1), 173-191 (1995).

*Table 1 – Common parameters in the eleven test cases.*

Parameter	Value
Source heights (measured from ground surface directly below)	10, 40, 100, and 400 m
Source noise and performance data (developed from AEDT/INM source data)	747-400 overflight at 7444 lbs thrust
Receiver height (above the ground surface)	1.219 m
Effective flow resistivities (soft ground, hard ground)	150 and 20,000 cgs Rayls
Temperature	14.9 °C
Noise metric	A-weighted max. sound level

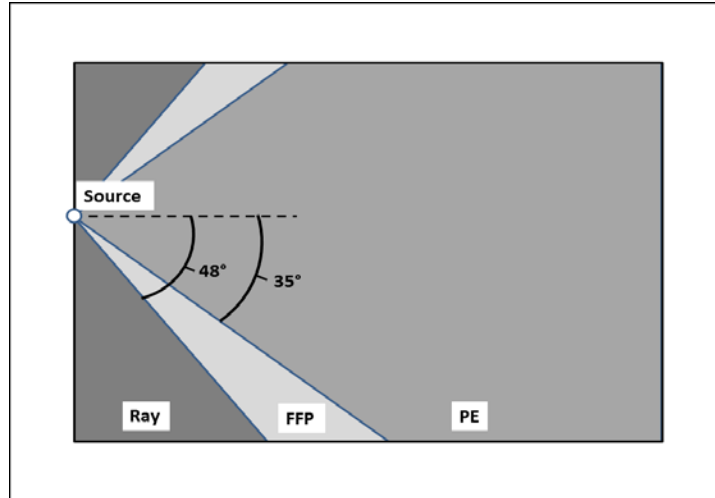


Fig. 1 - Combination of component models in HPM in the vertical plane.

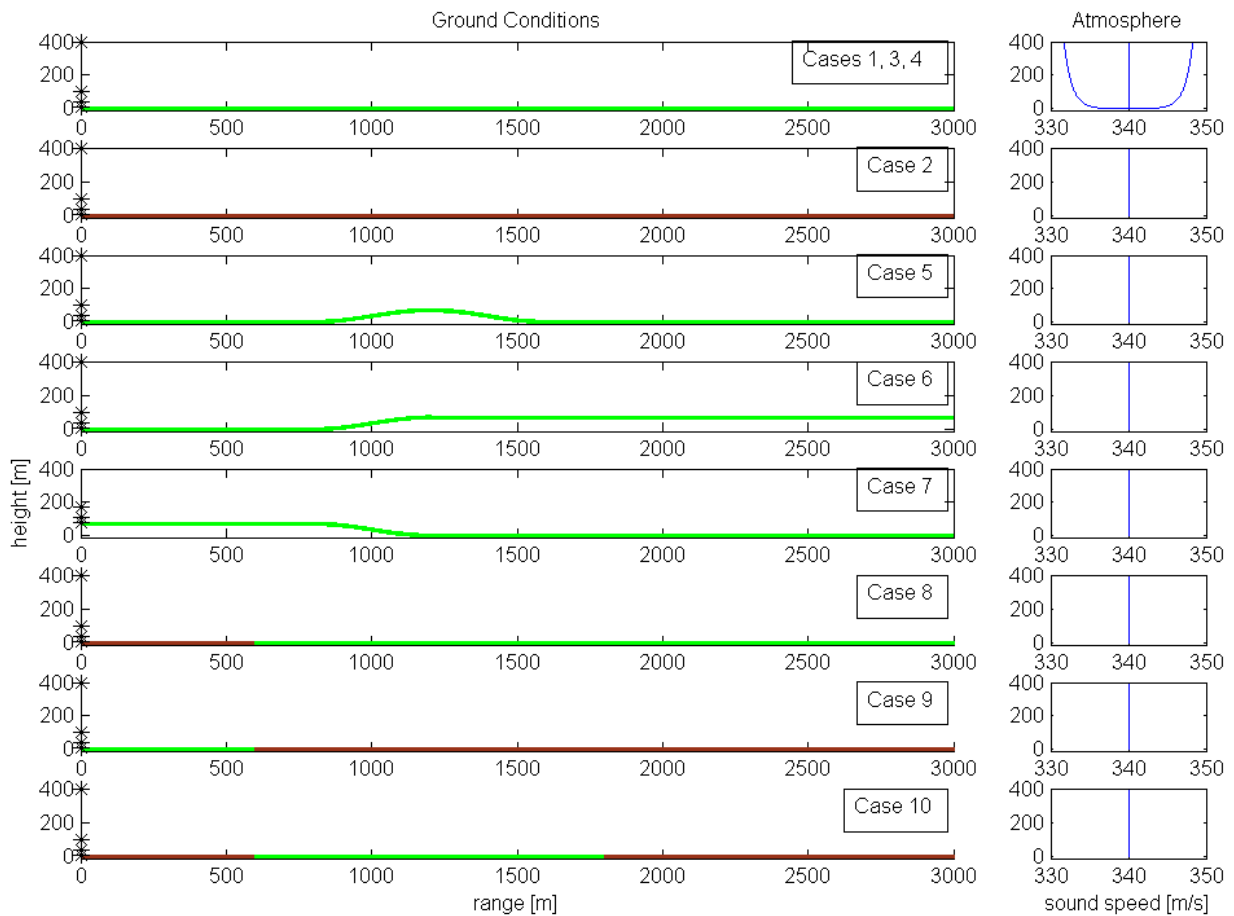


Fig. 2 - Diagrams of the ground and atmospheric conditions of the eleven test cases (green lines indicate soft ground, brown lines hard ground).

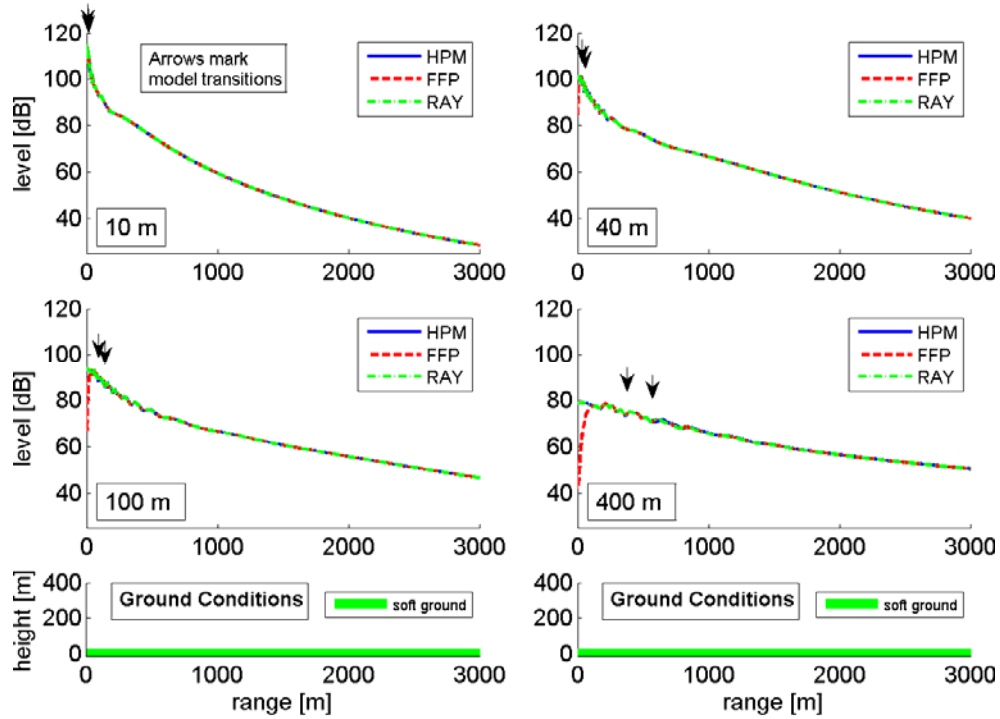


Fig. 3 - Case 1: Baseline. HPM, FFP, and RAY results compared for each source height: 10 m, 40 m, 100 m, and 400 m. Arrows indicate transition points between components of the HPM. A diagram of the propagation conditions is included beneath the results figures.

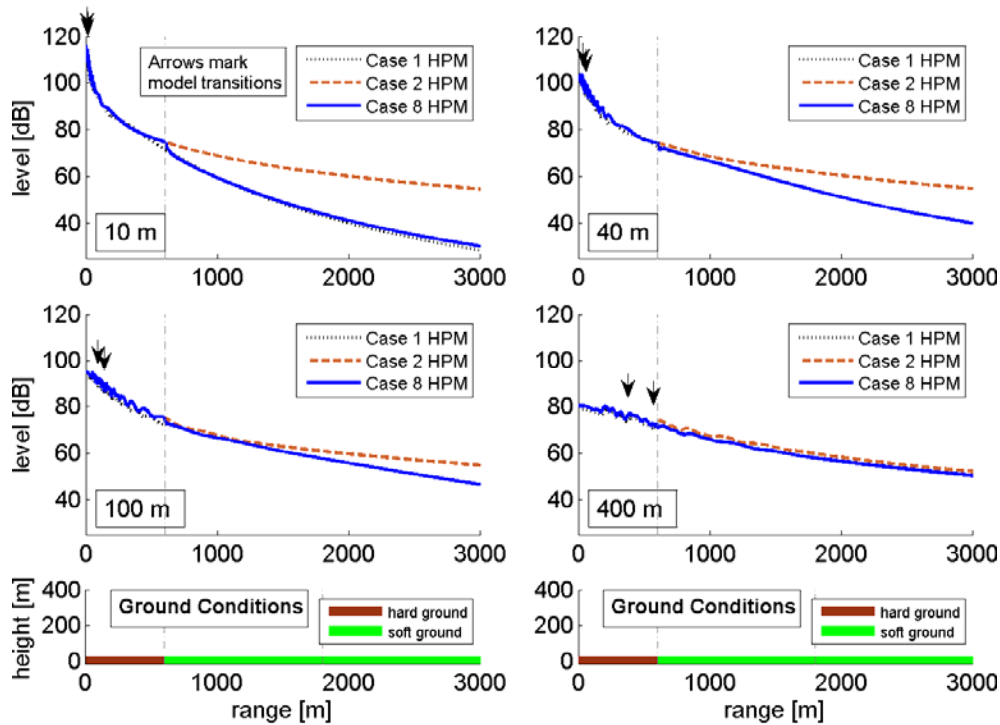


Fig. 4 - Case 8: Hard to soft ground transition with flat terrain and homogeneous atmosphere. HPM results are shown for each source height: 10 m, 40 m, 100 m, and 400 m.

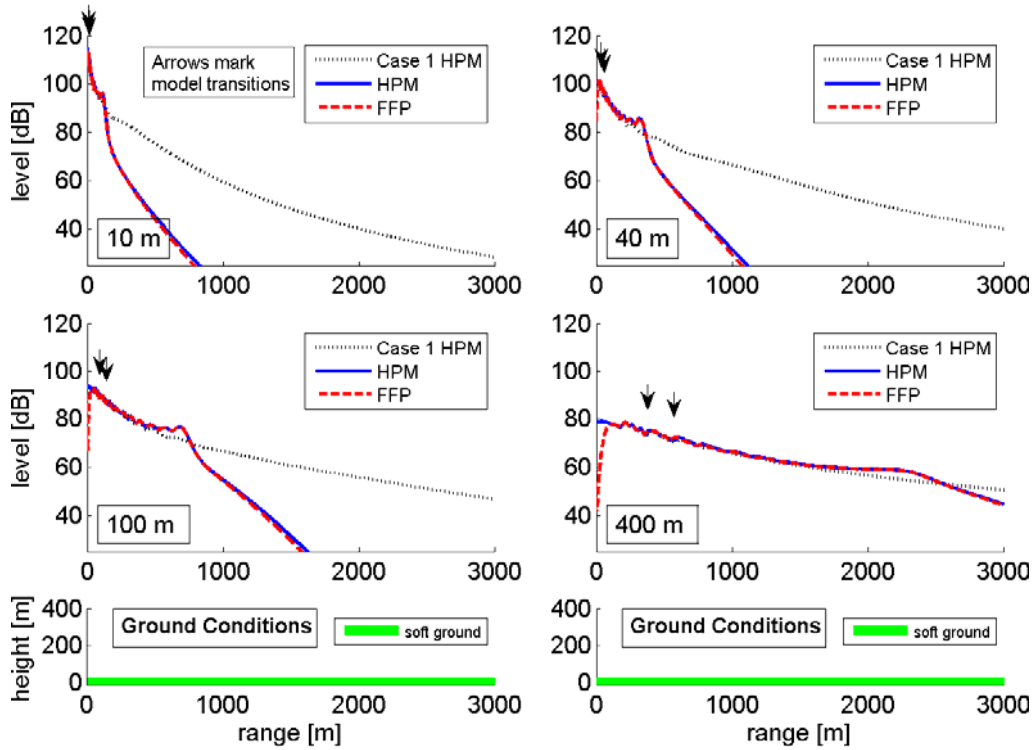


Fig. 5 - Case 3: Soft, flat ground and an upward refracting atmosphere. HPM and FFP results are compared for each source height: 10 m, 40 m, 100 m, and 400 m.

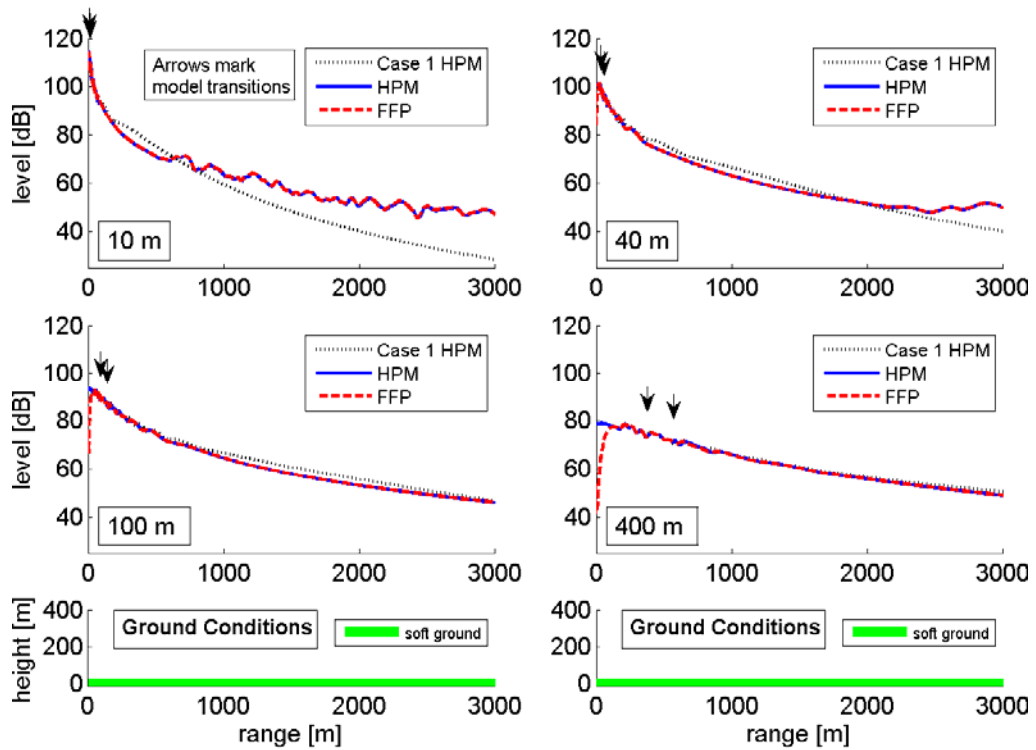


Fig. 6 - Case 4: Soft, flat ground and a downward refracting atmosphere. HPM and FFP results are compared for each source height: 10 m, 40 m, 100 m, and 400 m.

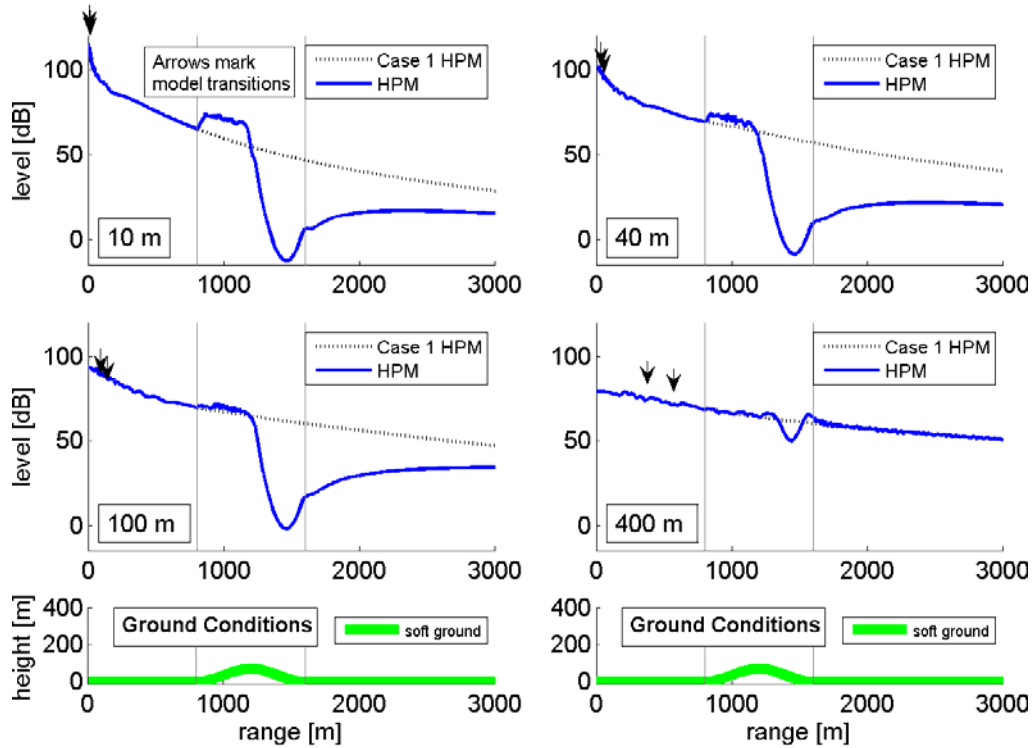


Fig. 7 - Case 5: Soft ground with hill terrain and homogeneous atmosphere. HPM results are compared for each source height: 10 m, 40 m, 100 m, and 400 m.

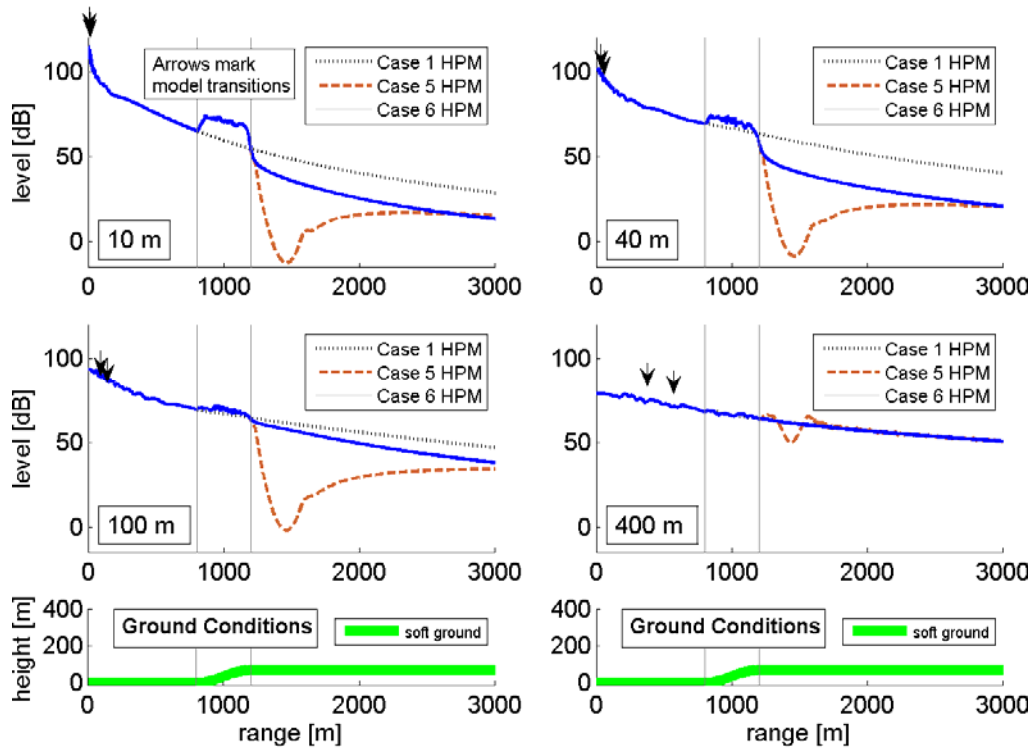


Fig. 8 - Case 6: Soft ground with upward sloping terrain and homogeneous atmosphere. HPM results are compared for each source height: 10 m, 40 m, 100 m, and 400 m.